Raman spectra of c-$Si_{1-x}Ge_x$ alloys

M. I. Alonso and K. Winer*
Max-Planck-Institut für Festkörperforschung, Heisenbergstrasse 1, D-7000 Stuttgart 80, Federal Republic of Germany
(Received 25 July 1988; revised manuscript received 15 November 1988)

We observe several weak features between 420 and 470 cm^{-1} in addition to the normally observed Si-Si ($\sim$500 cm^{-1}), Si-Ge ($\sim$400 cm^{-1}), and Ge-Ge ($\sim$300 cm^{-1}) optic modes in the Raman spectra of $Si_{1-x}Ge_x$ ($0.28 \leq x \leq 0.77$) single crystal layers grown by liquid-phase epitaxy (LPE). The quasiequilibrium LPE-growth process rules out the type of long-range ordering recently observed in $Si_{1-x}Ge_x$/Si strained-layer superlattices as the origin for these peaks. Calculations of the first-order Raman spectra of random 216-atom c-$Si_{1-x}Ge_x$ alloys reproduce these weak features, which proves that they are not due to second-order Raman processes. Normal-mode analysis shows that they are due to localized Si-Si motion in the neighborhood of one or more Ge atoms. Implications for strain-induced long-range ordering in c-$Si_{1-x}Ge_x$ alloys are discussed.

I. INTRODUCTION

Strained-layer superlattices derive their name from their high built-in strains that, through the nonequilibrium molecular-beam-epitaxial- (MBE-) growth process, allow the accommodation of large (4.2% for Ge on Si) lattice-constant mismatches without the introduction of misfit dislocations.[1] The presence of high strain in the $Si_{1-x}Ge_x$/Si strained-layer superlattice system has been shown[2] to lead to an ordering transition under certain annealing conditions, which results in the long-range ordering of alloy layers into single-atom type (111) planes in the sequence SiSiGeGeSiSiGeGe. . . as evidenced by extra Laue reflections in their electron-diffraction patterns.

Lockwood *et al.*[3] have presented additional possible evidence for this type of long-range ordering in $Si_{1-x}Ge_x$/Si ($0.2 \leq x \leq 0.5$) strained-layer superlattices. They found several weak Raman peaks in addition to the normally observed Si-Si (500 cm^{-1}), Si-Ge (400 cm^{-1}), and Ge-Ge (300 cm^{-1}) optic LO-TO modes[4] in c-$Si_{1-x}Ge_x$/Si superlattices in which the extra Laue reflections characteristic of long-range ordering were observed. However, Lockwood *et al.* also observed these extra reflections and extra weak Raman peaks in a relaxed 1-μm-thick single epitaxial layer of $Si_{0.8}Ge_{0.2}$/Si, which rules out strain as the driving force behind the long-range-ordering transition. Because their simple lattice-dynamics calculation for the ordered phase could reproduce both the frequencies of the weak Raman peaks and their shift with changing alloy composition, Lockwood *et al.* concluded that weak long-range ordering caused by the MBE-growth process was directly responsible for these peaks, although they noted the observation of similar weak peaks in the Raman spectra of bulk polycrystalline $Si_{1-x}Ge_x$ alloys.[4,5]

Recently, we have described the growth of single-crystal $Si_{1-x}Ge_x$ alloy layers on Si(111) substrates by liquid-phase epitaxy (LPE),[6] where the crystals are grown from a saturated Si-Ge-In solution by slow cooling. In contrast to MBE, the LPE-growth process always takes place close to thermodynamic equilibrium. No microscopically ordered structure is expected to be stable under this condition,[7] so that $Si_{1-x}Ge_x$ alloys grown by LPE should have a random distribution of Si and Ge atoms. Microprobe analysis in different points of our samples confirmed constant local composition.[6] We obtained this same result for bulk polycrystalline alloys grown from Si-Ge melts, which are known to undergo no phase changes even after prolonged annealings.[8] Extended x-ray-absorption fine-structure (EXAFS) measurements in c-$Si_{1-x}Ge_x$ (Ref. 9) indicate that Si and Ge atoms are randomly mixed; c-$Si_{1-x}Ge_x$ is a true random alloy. This is due to the small ionicity of the Si—Ge bond[7] and is in contrast with findings in other semiconductor alloys: Fine structure has been observed[10] in the infrared lattice-vibration spectra of $GaAs_xP_{1-x}$ alloys, which implies a tendency to clustering of like anions on their sublattice. Examples in other alloy systems, where first-order infrared absorption by weak extra modes was found, are given by Barker and Sievers,[11] who have reviewed the subject of optical studies of lattice vibrations of mixed crystals. Stability of different microscopic atomic structures for different alloy systems has been studied theoretically applying first-principles methods.[7,12,13] In particular, it is expected[13] that $GaAs_xSb_{1-x}$ deviates from the random distribution as described above for $GaAs_xP_{1-x}$.

Here we present Raman spectra for several $Si_{1-x}Ge_x$ single-crystal layers grown by LPE which exhibit the same weak Raman peaks observed by Lockwood *et al.* A realistic lattice-dynamics calculation in compositionally random c-$Si_{1-x}Ge_x$ shows that first-order Raman scattering by optic phonons associated with Si-Si motion in the nearest neighborhood of several Ge atoms is responsible for these weak extra Raman peaks.

II. SAMPLE PREPARATION AND EXPERIMENTAL CONSIDERATIONS

The three c-$Si_{1-x}Ge_x$/Si(111) ($x=0.28$, 0.55, and 0.77) samples used in this study were grown from Si-Ge-

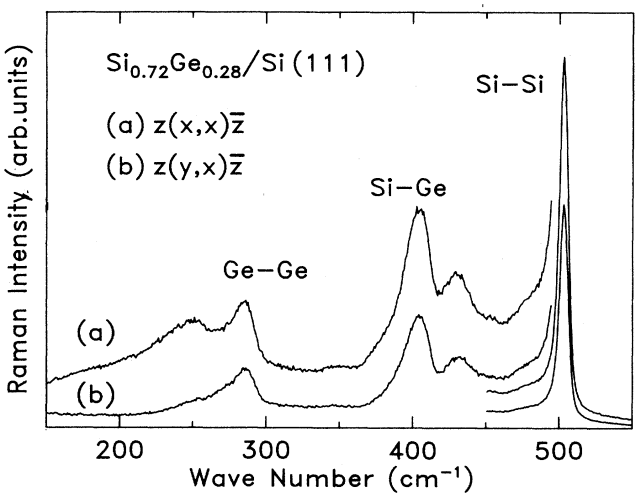

FIG. 1. Raman spectra measured at room temperature in two different backscattering configurations in a LPE-grown $Si_{0.72}Ge_{0.28}$/Si (111) layer. The crystal axes x, y, and z are defined as $x\|[1,\bar{1},0]$, $y\|[1,1,\bar{2}]$, and $z\|[1,1,1]$. The Raman-intensity scale is linear.

In solutions saturated at 900 °C for $x=0.28$ and 640 °C for $x=0.55$ and 0.77. The resulting alloy layers were between 1 and 5 μm thick. We determined their composition by measuring their lattice constants[13] using the (333) x-ray-diffraction peaks and assuming that they were completely relaxed (no residual strain due to the lattice mismatch between layer and substrate). This assumption is confirmed by the positions of the Si-Si, Si-Ge, and Ge-Ge Raman peaks, which agree with bulk polycrystalline SiGe alloys of corresponding compositions.[4,14] The Raman measurements were performed at room temperature in the backscattering configuration. Spectra were taken for incident and scattered light polarized both parallel or perpendicular to each other. The depolarization ratio is roughly 2:3, as shown in Fig. 1 for a sample with $x=0.28$, which corresponds to the selection rules for diamond,[15] except for the low-frequency part of the spectrum. This behavior is characteristic for all the investigated compositions. The spectra were excited with the 514.5-nm line of an Ar^+ laser. The scattered light was dispersed in a triplemate spectrometer and detected by optical multichannel techniques with a spectral resolution of 5 cm^{-1}.

III. RESULTS OF THE RAMAN MEASUREMENTS

In Fig. 2 we present the unpolarized room-temperature Raman spectra of LPE-grown single crystal layers of $Si_{1-x}Ge_x$/Si for three representative compositions $x=0.28$, 0.55, and 0.77. Peak positions for these three compositions are given in Table I. Each spectrum is characterized by three dominant peaks centered near 300, 400, and 500 cm^{-1}. These correspond to scattering from optic phonons involving Ge—Ge, Si—Ge, and Si—Si stretching motions, respectively. The origin of these peaks is well understood,[4] and their frequency dependence as a function of composition has been calculated[16]

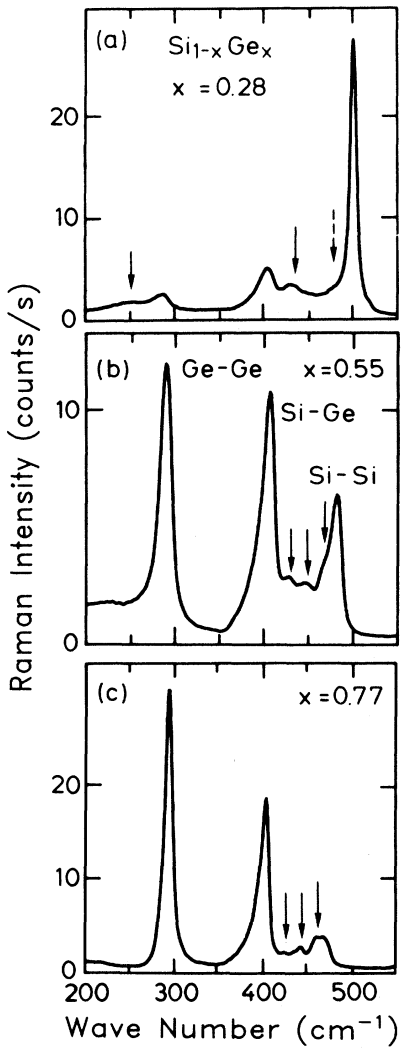

FIG. 2. Raman spectra measured for three single-crystal $Si_{1-x}Ge_x$ alloy layers grown by liquid-phase epitaxy with the following compositions: (a) $x=0.28$, (b) $x=0.55$, and (c) $x=0.77$. Arrows denote the weak extra Raman peaks.

with an isodisplacement model.[11] In addition to these peaks, each spectrum contains one or more weak contributions between 420 and 470 cm^{-1}. These contributions are best resolved (into peaks centered at 428 and 446 cm^{-1}, and a weak shoulder at 468 cm^{-1}) for $x=0.55$ [see Fig. 2(b)]. Only three modes were obtained in Ref. 16 be-

TABLE I. Peak frequencies for the main Raman-active modes measured for LPE-grown single-crystal $Si_{1-x}Ge_x$ alloy layers for the three compositions $x=0.28$, 0.55, and 0.77. The weak peaks given in parentheses correspond to the observed shoulder close to the Si-Si peak. The frequencies are in units of cm^{-1}.

x	Ge-Ge	Si-Ge	Si-Si	Weak peaks
0.28	287	404	502	247, 430
0.55	290	407	482	428, 446 (468)
0.77	295	404	468	424, 443 (459)

cause only three independent coordinates were considered.

The peak frequencies above 390 cm^{-1} of the LPE-grown single-crystal $Si_{1-x}Ge_x$ alloy layers are compared to those of bulk polycrystalline $Si_{1-x}Ge_x$ alloys as a function of Ge content x in Fig. 3. The fact that the frequency dependence on x for both sets of samples is the same shows that the former alloy layers are free of strain. The Si-Si peak frequency varies linearly with composition ($\omega_{Si\text{-}Si} \simeq 520-70x$), while the Si-Ge peak frequency varies slowly over most of the composition range, in agreement with previous results.[4] We believe that the nonlinearity of the Si-Si peak versus x observed in Refs. 4 and 17 is due to the proximity of a weak peak, stronger than the Si-Si peak for $x > 0.75$. The three weak extra peaks display similar behavior; the highest-frequency peak (~ 460 cm^{-1}) tracks the Si-Si frequency over most of its limited range while the lowest-frequency weak peak (~ 430 cm^{-1}) varies slowly with x, like the Si-Ge peak. The compositional dependence of the third weak-peak frequency is an average of the latter two. This similarity suggests that the ~ 430- and ~ 460-cm^{-1} weak extra peaks are related to (or derived from) the Si-Ge and Si-Si phonon bands, respectively.

There is only one additional peak between 420 and 470 cm^{-1} in the Raman spectrum for $x = 0.28$ centered at 430 cm^{-1} [see Fig. 2(a)]. A weak shoulder marked by a dashed arrow seems to be present, but it is not clearly resolved. There is also an additional weak feature at 247 cm^{-1} which has been previously observed in bulk polycrystalline $Si_{1-x}Ge_x$ alloys and has been attributed to a resonant mode.[17] Measurements as a function of alloy composition show that the observed peak is a composite peak. While for Ge-rich alloys two separate broad peaks around 170 cm^{-1} (2TA) (Ref. 18) and 200 cm^{-1} are observed, in the range of compositions $x = 0.15$ to 0.40 the two peaks overlap, giving rise to the apparently sharp peak at 247 cm^{-1}. In our (111)-oriented samples this low-energy structure is only observable for parallel polarizations of incident and scattered light, and it disappears almost completely for crossed polarizations, as shown in Fig. 1, which indicates that the corresponding Raman tensor has predominantly Γ_1 symmetry.[15] The selection rules for Raman scattering in compositionally disordered c-SiGe alloys need not be the same as in c-Si or c-Ge. However, the decomposition of the Raman spectrum of c-$Si_{0.7}Ge_{0.3}$/Si(100) into its different symmetry components is similar to that for c-Si and c-Ge,[19] suggesting that diamond-structure selection rules are essentially preserved in c-$Si_{1-x}Ge_x$ alloys. Therefore, we conclude that the feature at 247 cm^{-1} in Fig. 1(a) is due in part to second-order Raman scattering (Γ_1 as opposed to $\Gamma_{25'}$ symmetry in first order), although both weak $\Gamma_{25'}$ and disorder-induced Γ_1 first-order contributions cannot be entirely ruled out.

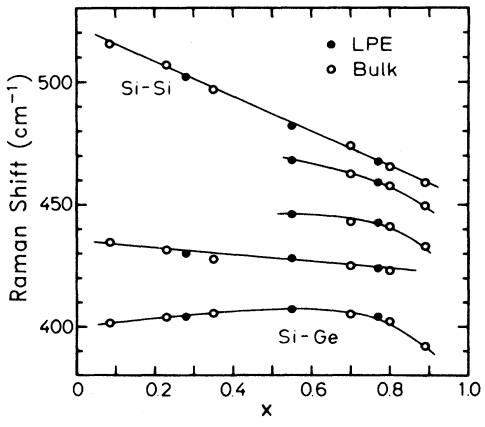

FIG. 3. Positions of the weak peaks observed between 420 and 470 cm^{-1} in LPE single-crystal and bulk polycrystalline $Si_{1-x}Ge_x$ alloys as a function of Ge content x. The feature close to the Si-Si peak (~ 460 cm^{-1}) is observed as a shoulder that becomes larger than this peak for $x > 0.75$. The solid lines are drawn as a guide to the eye.

The features in Fig. 2(a), including the additional weak peaks, are virtually identical to those for the 20% Ge MBE-grown single epitaxial layer of c-$Si_{1-x}Ge_x$/Si measured by Lockwood *et al.*[3] Thus, their claim that weak long-range order is directly responsible for the additional peaks in the Raman spectrum at 250 and 430 cm^{-1} cannot be correct; the equilibrium LPE-growth process precludes such long-range order. The presence of similar additional peaks in the Raman spectra of polycrystalline $Si_{1-x}Ge_x$ bulk alloys has been previously observed,[4,5,17] but their origin has not yet been established. Brya[5] proposed that these minor peaks are local (resonant) modes of Si(Ge) impurities in the Ge-(Si-) rich alloys. Lannin[17] suggested that the 200–250-cm^{-1} peak is a resonant mode for $x \leq 0.4$, while for higher Ge contents its character changes to disorder-induced LA scattering. A simple, though realistic, lattice-dynamics calculation can resolve the question of the origin of these additional peaks.

IV. MODELING THE RAMAN SPECTRA

We use a 216-atom cubic supercell ($a_0 = 16.2813$ Å) of Si in the diamond structure and randomly replace Si atoms by Ge ones until the desired composition is achieved. In this way we obtain nearly perfect random distributions of Si and Ge atoms in the supercell; that is, in all the studied cases the probability of occurrence of Si—Si, Si—Ge, and Ge—Ge bonds in the supercell is close to $(1-x)^2$, $2x(1-x)$, and x^2, respectively. For example, in the supercell generated for $x = 0.50$ we found the probabilities 0.243, 0.514, and 0.243, instead of 0.25, 0.50, and 0.25 in the ideally random case. Because of the difference in ideal-crystal bond lengths ($r_{Si\text{-}Si}/r_{Ge\text{-}Ge} = 2.35/2.46$) or, equivalently, lattice constants, we allow the cubic unit cell to adjust its shape by varying the three "orthorhombic" lattice constants a_{xx}, a_{yy}, and a_{zz}. For each new set of lattice constants, we allow the coordinates of the 216 atoms to relax to their minimum Keating potential-energy configuration.[20] We choose that set of lattice constants whose relaxed configuration has the lowest Keating potential energy for the final structure and repeat this procedure for all three ($x = 0.28$, 0.55, and 0.77) Ge concentrations. We further employ the

Keating potential to construct and diagonalize the dynamical matrix and thereby obtain the $\mathbf{k}=\mathbf{0}$ phonon density of states and eigenvectors for each composition. We use the following force constants: $\alpha_{\text{Si-Si}}=39.5$ N/m, $\alpha_{\text{Ge-Ge}}=35.0$ N/m, and $\beta/\alpha=0.285$ (Ref. 21) for all bond pairs, the former two being fitted to reproduce the single LO-TO Raman mode in c-Ge and c-Si at 301 and 520 cm^{-1}, respectively. The force constants α give essentially the elastic energy due to changes in bond lengths, while β takes into account changes in bond angles. Both $\alpha_{\text{Si-Ge}}$ and $r_{\text{Si-Ge}}$ are taken to be the geometric mean of the corresponding pure crystalline values. Finally, we calculate the first-order Raman spectrum for each structure by applying the following phenomenological model for the three independent components of the Raman polarizability due to Alben *et al.*,[22]

$$\vec{\alpha}_1=\sum_{l=1}^{N}\sum_{i=1}^{4}(\hat{\mathbf{r}}_{li}\cdot\hat{\mathbf{r}}_{li}-\vec{\mathbf{I}}/3)\mathbf{u}_l\cdot\hat{\mathbf{r}}_{li}\ , \tag{1}$$

$$\vec{\alpha}_2=\sum_{l=1}^{N}\sum_{i=1}^{4}[\tfrac{1}{2}(\hat{\mathbf{r}}_{li}\cdot\mathbf{u}_l+\mathbf{u}_l\cdot\hat{\mathbf{r}}_{li})-\vec{\mathbf{I}}/3]\mathbf{u}_l\cdot\hat{\mathbf{r}}_{li}\ , \tag{2}$$

$$\vec{\alpha}_3=\sum_{l=1}^{N}\sum_{i=1}^{4}\vec{\mathbf{I}}\mathbf{u}_l\cdot\hat{\mathbf{r}}_{li}\ , \tag{3}$$

where N is the number of atoms, $\mathbf{u}_l$ the eigenvector of atom l for a given vibrational mode, $\vec{\mathbf{I}}$ the unit dyadic, and $\hat{\mathbf{r}}_{li}$ the unit bond vector from atom l to atom i. The tensor $\vec{\alpha}_1$ corresponds to changes in the polarizability due to pure stretching motions and gives rise to the sole first-order Raman peak in c-Si at 520 cm^{-1}, whereas $\vec{\alpha}_2$ and $\vec{\alpha}_3$ vanish in the case of perfectly symmetric tetrahedral bonding. In our case, the departure from tetrahedral symmetry is small, and, therefore, we expect $\vec{\alpha}_1$ to be the dominant mechanism. We define the Raman intensity for each eigenmode as

$$I\propto\frac{n+1}{N\omega}\tfrac{1}{3}(\alpha_{1xy}^2+\alpha_{1xz}^2+\alpha_{1yz}^2)\ , \tag{4}$$

where n is the Bose-Einstein statistical factor and ω the eigenfrequency. In Eq. (4) we take an average of the significant elements of $\vec{\alpha}_1$ to avoid anisotropies due to the finite size of the supercell. In calculations of the high-frequency ($\omega>400$ cm^{-1}) weak peaks, we can ignore the $\vec{\alpha}_2$ and $\vec{\alpha}_3$ contributions because they are a factor of $\sim 10^3$ smaller than that of $\vec{\alpha}_1$. However, because $\vec{\alpha}_3$ corresponds to totally polarized (Γ_1 symmetry) Raman scattering which characterizes the low-frequency ($\omega\leq 250$ cm^{-1}) weak peaks, we expect this mechanism [$I\propto(n+1)N^{-1}\omega^{-1}\alpha_3^2$] to contribute strongly to any disorder-induced first-order scattering in this spectral region.

A. Modeling results for random alloys

In Fig. 4 we show the results of the calculation for the three Ge concentrations ($x=0.28$, 0.55, and 0.77) whose Raman spectra are shown in Fig. 2. Each calculated spectrum corresponds to the phonon density of states with the weight for each mode equal to its calculated Raman intensity I [Eq. (4)]. In each case, there is good qualitative agreement between the calculated and measured Raman spectra. Even the weak additional Raman peaks between 420 and 470 cm^{-1} are clearly present in the calculated spectra, except for the highest Ge concentration, where they are either too weak to be observed or masked by neighboring peaks. The Raman spectra above the Si-Ge peak are essentially given by the phonon density of states. The calculated peak positions differ slightly from the measured ones, but this could be remedied by adjusting several available free parameters in the Keating model (i.e., β_{SiGeSi}, β_{SiSiGe}, etc.) for a more quantitative fit. However, this is not necessary to prove that first-order Raman processes in compositionally random c-$Si_{1-x}Ge_x$ alloys are sufficient to account for the extra weak peaks

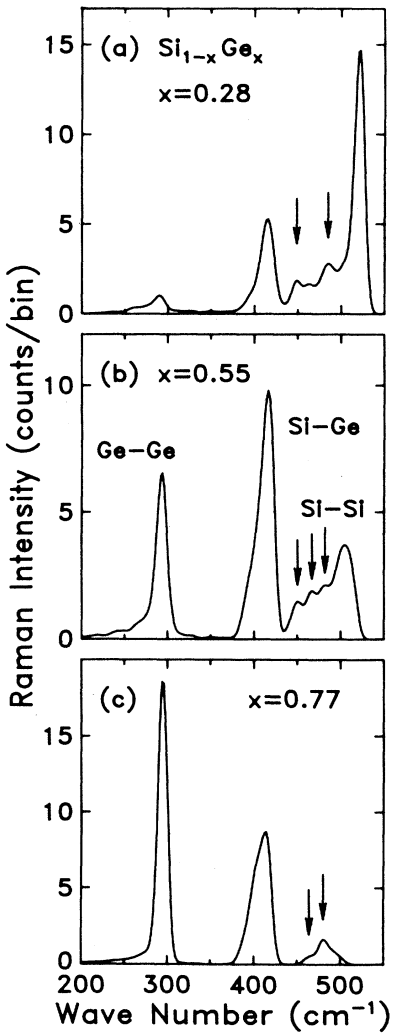

FIG. 4. Raman spectra calculated for three random c-$Si_{1-x}Ge_x$ alloys using a 216-atom supercell and the Keating potential for the following compositions: (a) $x=0.28$, (b) $x=0.55$, and (c) $x=0.77$. The calculated histograms (bin width 2 cm^{-1}) were smoothed by Gaussian broadening (full width at half maximum 5 cm^{-1}). The Raman-intensity units are arbitrary but the same for all calculated spectra.

of interest. Similar results for weak infrared modes were found using a quite different model for $GaAs_xP_{1-x}$.[10] Thus, neither second-order Raman scattering nor long-range ordering is required to explain the weak extra peaks between 420 and 470 cm^{-1} that appear in the Raman spectra of all c-$Si_{1-x}Ge_x$ samples, whether they are MBE or LPE grown, superlattices or single epitaxial layers, or bulk polycrystalline alloys.

In order to determine the origin of these weak extra peaks, we examine the eigenvectors of the corresponding normal modes. Because of the optic character of Raman-active phonons in c-Si and c-Ge, we intuitively expect that they involve the stretching of Si—Si bonds where one or more neighbors of either Si atom are replaced by Ge atoms. The larger mass of the neighboring Ge atom(s) should decrease the force constant that determines the Si—Si stretching frequencies, thus pulling modes out of the pure Si LO-TO band to lower frequencies. This effect should also contribute to the gradual reduction in the frequency of the Si-Si phonon band maximum with increasing Ge content.

In Fig. 5 we present a specific example of this behavior where we show the atomic motions for the mode with $\omega=468$ cm^{-1} calculated for the c-$Si_{0.45}Ge_{0.55}$ alloy. This mode provides the main contribution to the central weak extra Raman peak for this Ge concentration [see Fig. 4(b)]. The central Si atom vibrates mainly in the z direction while its two Si neighbors move along the bond directions. The two Ge atoms execute much smaller motions (4% of the central atom). Similar eigenmodes are observed at nearly the same frequency in the two other compositions as well. The resulting lower frequency can be understood with the following idealized model. We assume that only the silicon atoms move and that the germanium atoms are fixed ($m_{Si}/m_{Ge}\rightarrow 0$). The eigenfrequency ω is then determined by the effective stretching force constant κ_i for each bond and the mass of Si, m_{Si}. In the case that the central Si has four Si neighbors, ω_0 would be given by

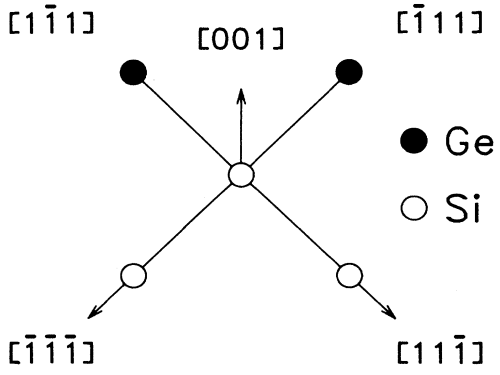

FIG. 5. Schematic normal-mode displacements for $x=0.55$ and $\omega=468$ cm^{-1} as described in the text. Open circles depict Si, solid circles Ge.

$$\omega_0^2=(1/m_{Si})\sum_{i=1}^{4}\kappa_i=(\kappa_0/3m_{Si})(2+2+2+2)\ . \quad (5)$$

If two of the neighbors are replaced by Ge atoms, then the contribution from each of the two Si—Ge bonds to κ_i in Eq. (5) is 1 instead of 2, i.e.,

$$\omega^2=(\kappa_0/3m_{Si})(2+2+1+1)\ , \quad (6)$$

so that

$$\omega/\omega_0=\sqrt{3/4}=0.87\ . \quad (7)$$

Thus the frequency $\omega_0=520$ cm^{-1} in pure c-Si should be reduced by a factor of 0.87 to 450 cm^{-1}, in reasonable agreement with the calculated value of 468 cm^{-1} for the nearly ideal eigenmode depicted in Fig. 5.

The frequency of similar Si-Si Raman-active modes should decrease with one, two, or three Ge neighbors from 520 cm^{-1} to 486, 450, and 411 cm^{-1}, respectively, within this idealized model. The observed decrease in frequency of the Si-Si peak maximum with increasing Ge content is due in part to the statistical effect of an increasing average number of Ge neighbors per Si atom, which reduces the mean frequency of the Si-Si Raman-active modes. The resulting shift of the Si-Si Raman peak to lower frequencies with increasing Ge content in random c-$Si_{1-x}Ge_x$ alloys by this mechanism is related to phonon-confinement (localization) effects which have been invoked to explain such shifts in short-period c-$Si_{1-x}Ge_x$ superlattices.[23] Of course, the idealized model discussed above ignores structural changes and changes in force constants as the composition is varied. These effects contribute only slightly to the frequency shifts with composition; the difference in force constants [$\alpha_{SiGe}/\alpha_{SiSi}=\sqrt{(35.0)(39.5)}/39.5=0.94$] is much smaller than the difference in atomic masses ($m_{Si}/m_{Ge}=0.39$).

Not all of the normal modes that make up the weak Raman peaks between 420 and 470 cm^{-1} are as simple and symmetric as the one depicted in Fig. 5. However, the origin of all of these weak extra peaks is the same. Namely, that random introduction of Ge atoms into an initially pure Si crystal reduces the local symmetry, which leads to the localization of Si-Si optic phonons (phonon confinement) in the Ge neighborhoods. The frequencies of these modes are reduced through the effect of the larger Ge mass, which pulls modes out of the main Si-Si optic-phonon band to lower frequencies. Our results confirm the interpretation of Brya[5] for dilute Ge:Si alloys, except that the origin of the weak peaks is the same for the entire compositional range. These effects depend upon the presence of *dis*order and should *not* be operative in an ordered SiGe alloy.

The interpretation of the low-frequency weak Raman peak observed at 247 cm^{-1} for $x=0.28$ is complicated by the possible overlap of the 2TA second-order scattering peak (at 240 cm^{-1} for this composition[18] with a disorder-induced first-order scattering Γ_1 contribution. However, at compositions $x>0.65$ we observe a clear separation of this peak into components centered near

170 cm^{-1} [2TA (Ref. 18)] and 200 cm^{-1}, which agrees with earlier observations.[17] The main contribution of $\vec{\alpha}_3$ is at low frequencies with maxima near 200 cm^{-1} for all three studied compositions, as illustrated in Fig. 6 for $x=0.55$. This suggests that the disorder-induced first-order contribution to the observed low-frequency weak extra Raman peaks is significant.

B. Modeling results for the ordered structure

The ordered structure of Ourmazd and Bean[2] consists of alternate pairs of Si and Ge(111) planes. The primitive unit cell has axes $(a/2)[110]$, $(a/2)[011]$, and $a[101]$, and contains two Si and two Ge atoms. We have constructed a supercell of 64 atoms corresponding to 16 of these primitive unit cells and have calculated the frequencies and the eigenvectors for the relaxed coordinates. There are four symmetry-allowed Raman-active modes which occur at 84, 281, 426, and 483 cm^{-1}, as shown in Fig. 7. Eigenvectors for the four modes are also shown schematically in Fig. 7. The modes consist of phonons with atomic motions either along (281 and 483 cm^{-1}) or perpendicular to (84 and 426 cm^{-1}) the $\langle 111 \rangle$ directions.

The Raman spectrum for a c-$Si_{0.5}Ge_{0.5}$ random alloy also contains three dominant peaks whose calculated frequencies are shown by arrows in Fig. 7. The superlattice peak at 281 cm^{-1} cannot be identified with the peak at 247 cm^{-1} in Fig. 1 because of its observed polarization dependence. We must also note that the peaks calculated in the Raman spectrum of the ordered structure are higher than their random-alloy counterparts [compare with Fig. 4(b)]. The integrated Raman intensity in both cases is about the same, but in the disordered (random) alloys it is spread over many modes that are hence broader and of reduced height. A similar effect in the $\vec{\alpha}_1$ Raman intensity [Eq. (1)] due to disorder from that in perfect diamond-structure Si crystal also occurs in the pure amorphous Si phase.[24]

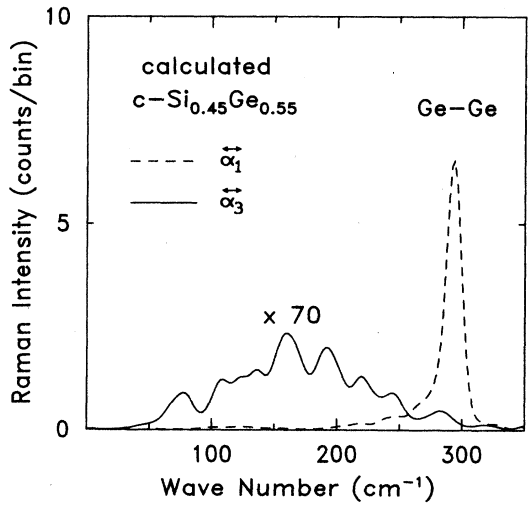

FIG. 6. Raman spectrum calculated for a random c-$Si_{0.45}Ge_{0.55}$ alloy, showing the totally polarized part $\vec{\alpha}_3$ in comparison to the dominant contribution $\vec{\alpha}_1$.

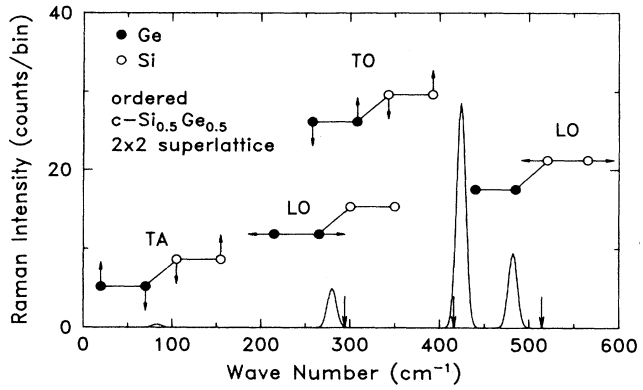

FIG. 7. Raman spectrum calculated for the ordered c-$Si_{0.50}Ge_{0.50}$ alloy. Representative eigenvectors for the four Raman-acitve modes are also shown. Calculated peak positions for a random c-$Si_{0.50}Ge_{0.50}$ alloy are marked by arrows. The Raman-intensity units are the same as in Fig. 4.

No additional weak peaks are allowed in the perfectly ordered structure. The reduced frequency of the Si—Si stretching mode to 483 cm^{-1} is due to the same confinement effect caused by the much larger mass of the Ge atoms that gives rise to the weak extra Raman peaks in the random alloys. No other peaks near this frequency are possible because each and every Si atom has three Ge neighbors. If deviations from perfect ordering are present, additional weak Raman peaks appear as the average number of Ge neighbors per Si atom is reduced from three. Thus the presence of weak extra Raman peaks in the spectrum is the signature for compositional *dis*order and localization rather than long-range order, and their relative intensity should provide a useful measure of order for the characterization of c-SiGe alloys. The interpretation of the Raman spectrum for a c-SiGe alloy with a mixture of a random plus a long-range-ordered phase has to take into account that the random phase gives rise to weak extra peaks. The fact that the intensities of the weak extra Raman peaks between 420 and 470 cm^{-1} in MBE-grown[3] c-$Si_{1-x}Ge_x$/Si superlattices whose electron-diffraction patterns exhibit extra reflections and those in LPE-grown c-$Si_{1-x}Ge_x$/Si alloys or bulk c-$Si_{1-x}Ge_x$ alloys grown from a melt[4,5,17] are nearly identical suggests that long-range ordering in the former, if it exists at all, must be extremely weak.

V. SUMMARY AND CONCLUSIONS

The original claim for a long-range-ordering transition in MBE-grown c-$Si_{1-x}Ge_x$/Si strained-layer superlattices by Ourmazd and Bean[2] was based primarily on the observation of extra reflections in the electron-diffraction patterns of these structures after certain annealing schedules. Because annealing was critical to the onset of ordering, Ourmazd and Bean suggested that the transition might be strain driven. Lockwood *et al.*[3] used dark-field imaging and electron diffraction to observe the same extra reflections in similar materials further supporting this claim. However, Lockwood *et al.* also ob-

served this behavior in a single 1-μm-thick epitaxial layer and failed to observe any dependence of these extra reflections on annealing conditions. The former result rules out strain as the driving mechanism for the order-disorder transition while the latter places the very existence of this transition in some doubt. Lastly, Lockwood *et al.* suggested that the weak extra Raman peaks observed in their *c*-SiGe/Si superlattices and *c*-SiGe single epilayer were signatures of the long-range ordering inferred from the electron-diffraction patterns of these same alloys.

In the present study we have shown that LPE-grown SiGe single-crystal layers as well as SiGe bulk polycrystals, where long-range order is precluded by the quasiequilibrium growth conditions, also exhibit the same weak extra Raman peaks observed in the Raman spectra of the MBE-grown c-$Si_{1-x}Ge_x$/Si structures in which long-range ordering was inferred by Lockwood *et al.* We have shown that these extra peaks are present in compositionally random alloys and are composed of localized Si-Si optic modes whose frequencies are lowered because of the larger mass of neighboring Ge atoms. We have also shown that the superposition of spectra of random and ordered *c*-SiGe phases is neither required nor able to account for the weak extra Raman peaks observed in all c-$Si_{1-x}Ge_x$ alloys, independent of the growth method.

Our results not only remove secondary support for the claim of a long-range-ordering transition in c-$Si_{1-x}Ge_x$/Si alloys, but they are apparently contradictory with previous results of Raman and electron-diffraction experiments (Ref. 3). Further work is needed to reconcile all observations: We suggest that a convincing test of the presence of nearly ideal long-range ordering in c-$Si_{1-x}Ge_x$/Si superlattices or alloys would be to measure the Raman spectrum for an alloy structure which exhibits very strong forbidden reflections in its electron-diffraction pattern.[25] In such a material, any extra weak peaks between 420 and 470 cm^{-1} in the Raman spectrum of the ordered c-$Si_{0.5}Ge_{0.5}$ structure must be dwarfed by the dominant Raman-allowed optic modes, and therefore the resulting Raman spectrum should be unlike any Raman spectrum of a c-$Si_{0.5}Ge_{0.5}$ alloy heretofore measured.

ACKNOWLEDGMENTS

We thank M. Cardona for many enlightening discussions and a critical reading of the manuscript. One of us (K.W.) thanks the Alexander von Humboldt-Stiftung (Federal Republic of Germany) for generous financial support.

*Present address: Xerox Palo Alto Research Center, 3333 Coyote Hill Road, Palo Alto, CA 94304.

[1]J. C. Bean, Science **230**, 127 (1985).
[2]A. Ourmazd and J. C. Bean, Phys. Rev. Lett. **55**, 765 (1985).
[3]D. J. Lockwood, K. Rajan, E. W. Fenton, J.-M. Baribeau, and M. W. Denhoff, Solid State Commun. **61**, 465 (1987).
[4]M. A. Renucci, J. B. Renucci, and M. Cardona, in *Light Scattering in Solids,* edited by M. Balkanski (Flammarion, Paris, 1971), p. 326.
[5]W. J. Brya, Solid State Commun. **12**, 253 (1973).
[6]M. I. Alonso and E. Bauser, J. Appl. Phys. **62**, 4445 (1987).
[7]A. Qteish and R. Resta, Phys. Rev. B **37**, 1308 (1988).
[8]M. Hansen and K. Anderko, *Constitution of Binary Alloys,* 2nd ed. (McGraw-Hill, New York, 1958), p. 774.
[9]S. Minomura, K. Tsuji, M. Wakagi, T. Ishidate, K. Inoue, and M. Shibuya, J. Non-Cryst. Solids **59&60**, 541 (1983). This study was carried out using c-$Si_{1-x}Ge_x$ obtained by annealing of a-$Si_{1-x}Ge_x$ films. Such films crystallize by annealing without segregation, as shown by A. Morimoto, M. Kumeda, and T. Shimizu, *ibid.* **59&60**, 537 (1983), and their Raman spectra contain the weak peaks of interest [P. V. Santos (private communication)].
[10]H. W. Verleur and A. S. Barker, Jr., Phys. Rev. **149**, 715 (1966).
[11]A. S. Barker, Jr. and A. J. Sievers, Rev. Mod. Phys. **47**, Suppl. No. 2, S1 (1975).
[12]G. P. Srivastava, J. L. Martins, and A. Zunger, Phys. Rev. B **31**, 2561 (1985).
[13]A. Qteish, N. Motta, and A. Balzarotti, in Proceedings of the 19th International Conference on Physics and Semiconductors (unpublished).
[14]J. P. Dismukes, L. Ekstrom, and R. J. Paff, J. Phys. Chem. **68**, 3021 (1964).
[15]M. Cardona, in *Light Scattering in Solids II,* Vol. 50 of *Topics in Applied Physics,* edited by M. Cardona and G. Guntherödt (Springer, Berlin, 1982), p. 19.
[16]G. M. Zinger, I. P. Ipatova, and A. V. Subashiev, Fiz. Tekh. Poluprovodn. **11**, 656 (1977) [Sov. Phys.—Semicond. **11**, 383 (1977)].
[17]J. S. Lannin, Phys. Rev. B **16**, 1510 (1977).
[18]R. A. Logan, J. M. Rowell, and F. A. Trumbore, Phys. Rev. **136**, A1751 (1964).
[19]M. I. Alonso (unpublished). The (100) orientation allows a larger variety of polarization configurations to be measured than the (111) orientation.
[20]P. N. Keating, Phys. Rev. **145**, 637 (1966).
[21]R. M. Martin, Phys. Rev. B **1**, 4005 (1970).
[22]R. Alben, D. Weaire, J. E. Smith, Jr., and M. H. Brodsky, Phys. Rev. B **11**, 2271 (1975).
[23]J. Menéndez, A. Pinczuk, J. Bevk, and J. P. Mannaerts, J. Vac. Sci. Technol. B **6**, 1306 (1988).
[24]K. Winer, Phys. Rev. B **36**, 6072 (1987).
[25]J. Bevk, J. P. Mannaerts, L. C. Feldman, B. A. Davidson, and A. Ourmazd, Appl. Phys. Lett. **49**, 286 (1986).